Electronic Supplementary Material (ESI) for Physical Chemistry Chemical Physics.

Vibronic energy relaxation approach highlighting deactivation pathways in carotenoids

Vytautas Balevičius Jr.,[1] Arpa Galestian Pour,[2] Janne Savolainen,[3] Craig N. Lincoln,[2] Vladimir Lukes,[4] Eberhard Riedle,[5] Leonas Valkunas,[1,6] Darius Abramavicius,[1] and Jürgen Hauer[2]

[1)] *Department of Theoretical Physics, Faculty of Physics, Vilnius University, Sauletekio Ave. 9, build. 3, LT-10222 Vilnius, Lithuania*

[2)] *Photonics Institute, Vienna University of Technology, Gusshausstrasse 27, 1040 Vienna, Austria*

[3)] *Department of Physical Chemistry II, Ruhr-University Bochum, 44780 Bochum, Germany*

[4)] *Department of Chemical Physics, Slovak University of Technology, Radlinského 9, 81237 Bratislava, Slovakia*

[5)] *Lehrstuhl für BioMolekulare Optik, Ludwig-Maximilians-University, Oettingenstrasse 67, 80538 Munich, Germany*

[6)] *Center for Physical Sciences and Technology, Institute of Physics, Savanoriu Ave. 231, LT-02300 Vilnius, Lithuania*

I. INTRODUCTION

In the main article it was demonstrated how an in-depth quantum-mechanical treatment of vibrational cooling explains the pump–probe signal of β-carotene. Previous studies, relying on Global Target Analysis (GTA), explained qualitatively similar experimental findings by invoking S^* as another electronic state besides S_1. In this Electronic Supporting Information we give in detail the modeling approach used in the main article (Section II), the fitting procedure and the obtained static model parameters (Section III), and discuss the principles of GTA in contrast to the quantum-mechanical modeling (Section IV). The purpose of the latter discussion is not to compare the quality of different target models for carotenoids, as done in several previous studies[1,2]. Rather we show: i) how GTA-results on carotenoids lend themselves to misinterpretation in the presence of rapidly changing and heavily overlapping spectral components of the underlying pump–probe signal, and ii) how GTA highlights the successes and shortcomings of the vibrational cooling model. Lastly, the details of quantum chemical calculations are given in Section V.

II. OFF-DIAGONAL FLUCTUATION MODEL

To describe the processes of internal conversion and vibrational cooling in a unified manner, we take the following Hamiltonian of two electronic states, $|1\rangle$ and $|2\rangle$ ($|S_1\rangle$ and $|S_2\rangle$ in the main article), coupled to two harmonic oscillators, α and β, via mutually shifted potential energy surfaces:

$$
\begin{aligned}
H = |1\rangle\langle 1| \sum_{i=\alpha,\beta} \left(\frac{p_i^2}{2m_i} + \frac{m_i\omega_i^2}{2} q_i^2 \right) \\
+|2\rangle\langle 2| \sum_{i=\alpha,\beta} \left(\frac{p_i^2}{2m_i} + \frac{m_i\omega_i^2}{2} (q_i - d_i^{(21)})^2 + \omega^{(21)} \right) \qquad (1) \\
+ \sum_{i=1,2;\kappa} c_\kappa x_\kappa q_i + \sum_\kappa f_\kappa x_\kappa \left(|1\rangle\langle 2| + |2\rangle\langle 1| \right) \\
+ \sum_\kappa \left(\frac{p_\kappa^2}{2m_\kappa} + \frac{m_\kappa\omega_\kappa^2}{2} x_\kappa^2 \right). \qquad (2)
\end{aligned}
$$

Here, q_i denotes the coordinate of the i-th vibrational mode. The modes are coupled with strength c_κ to an infinite set of harmonic oscillators of the bath with coordinates x_κ and momenta p_κ. To make the model simpler the coupling strength is identical for both modes. This coupling, characterized by spectral density $C_c''(\omega) \propto \sum_\kappa c_\kappa^2 \delta(\omega - \omega_\kappa)$, leads to the vibrational relaxation within the system. The off-diagonal elements of the electronic subspace (the second term in the second line) are coupled to the oscillators of the bath with coupling strength f_κ. The coupling, characterized by the spectral density $C_f''(\omega) \propto \sum_\kappa f_\kappa^2 \delta(\omega - \omega_\kappa)$, induces the internal conversion dynamics.

Quantizing the vibrational modes associated with the system we define the states $|ab_i\rangle = |a_i\rangle|b_i\rangle$, where indices a/b indicate the number of quanta of the α/β mode in the i-th electronic state, with energies $\varepsilon_\alpha/\varepsilon_\beta$. We re-cast the Hamiltonian, Eq. (2), into the following form:

$$\begin{aligned} H = &\sum_{a,b} |ab_1\rangle\langle ab_1|(\varepsilon_\alpha a_1 + \varepsilon_\beta b_1) + |ab_2\rangle\langle ab_2|(\omega^{(21)} + \varepsilon_\alpha a_2 + \varepsilon_\beta b_2) \\ &+ \sum_{\kappa,a,b,i=1,2} c_\kappa x_\kappa \sqrt{a_i+1}\,(|ab_i\rangle\langle (a+1)b_i| + |(a+1)b_i\rangle\langle ab_i|) \\ &+ \sum_{\kappa,a,b,i=1,2} c_\kappa x_\kappa \sqrt{b_i+1}\,(|ab_i\rangle\langle a(b+1)_i| + |a(b+1)_i\rangle\langle ab_i|) \\ &+ \sum_{\kappa,a,b,a',b'} f_\kappa x_\kappa\,(\langle a_1|a'_2\rangle\langle b_1|b'_2\rangle|ab_1\rangle\langle a'b'_2| + \langle a_2|a'_1\rangle\langle b_2|b'_1\rangle|ab_2\rangle\langle a'b'_1|) \\ &+ \sum_\kappa \left(\frac{p_\kappa^2}{2m_\kappa} + \frac{m_\kappa\omega_\kappa^2}{2}x_\kappa^2\right). \end{aligned} \tag{3}$$

The equations of motion for the populations of states $|ab_i\rangle$ are derived from the quantum Liouville equation in as described in Ref.[3]. Essentially, they are of the second order with respect to the system–bath coupling and involve the secular and Markov approximations. The equations are of the following form:

$$\frac{\mathrm{d}}{\mathrm{d}t}n_{ab_i} = \left(\frac{\mathrm{d}}{\mathrm{d}t}n_{ab_i}\right)_f + \left(\frac{\mathrm{d}}{\mathrm{d}t}n_{ab_i}\right)_c, \tag{4}$$

where the first term describes the internal conversion dynamics and the second one describes the vibrational relaxation. The terms explicitly read:

$$\left(\frac{\mathrm{d}}{\mathrm{d}t}n_{ab_2}\right)_f = \sum_{a'b'} |\langle a_2|a'_1\rangle|^2|\langle b_2|b'_1\rangle|^2 \left[-k^f_{ab,a'b'}n_{ab_2} + k'^f_{ab,a'b'}n_{a'b'_1}\right];$$

$$\left(\frac{\mathrm{d}}{\mathrm{d}t}n_{ab_1}\right)_f = \sum_{a'b'} |\langle a_1|a'_2\rangle|^2|\langle b_1|b'_2\rangle|^2 \left[-k'^f_{a'b',ab}n_{ab_1} + k^f_{a'b',ab}n_{a'b'_2}\right]; \tag{5}$$

$$\begin{aligned} \left(\frac{\mathrm{d}}{\mathrm{d}t}n_{ab_i}\right)_c = &\\ &-(a_i k^c(\varepsilon_\alpha) + (a_i+1)k'^c(\varepsilon_\alpha) + b_i k^c(\varepsilon_\beta) + (b_i+1)k'^c(\varepsilon_\beta))\,n_{ab_i} \\ &+(a_i+1)k^c(\varepsilon_\alpha)n_{(a+1)b_i} + a_i k'^c(\varepsilon_\alpha)n_{(a-1)b_i} \\ &+(b_i+1)k^c(\varepsilon_\beta)n_{a(b+1)_i} + b_i k'^c(\varepsilon_\beta)n_{a(b-1)_i}. \end{aligned} \tag{6}$$

Here, we have defined two kinds of rate constants — those between the vibrational levels of different electronic states, k^f, and those between the neighboring vibrational levels of the same electronic state only, k^c. The latter are explicitly shown as downhill rates corresponding to the energy gap ε, $k^c(\varepsilon)$, or the complementary uphill rates $k'^c(\varepsilon)$. These rates are obtained from the Fourier transform of the bath correlation function[3], which is related to the corresponding spectral density $C''_{c/f}(\varepsilon)$ as

$$C_{c/f}(\varepsilon) = C''_{c/f}(\varepsilon)\left(\coth(\frac{\beta\varepsilon}{2}) + 1\right), \tag{7}$$

where $\beta = (\mathrm{k_B}T)^{-1}$ is the inverse temperature. The downhill rate is then $k^c(\varepsilon) = C_c(|\varepsilon|)$ and the uphill rate is $k'^c(\varepsilon) = C_c(-|\varepsilon|)$. To give the rates k^f, we first define the energy gap $\Delta_{ab,a'b'} = \omega^{(21)} + \varepsilon_\alpha(a_2 - a'_1) + \varepsilon_\beta(b_2 - b'_1)$. We then have the rates as $k^f_{ab,a'b'} = C_f(\Delta_{ab,a'b'})$ and $k'^f_{ab,a'b'} = C_f(-\Delta_{ab,a'b'})$.

In order to describe the dynamics within the carotenoid S_1 and S_2 states, which are represented by the states $|1\rangle$ and $|2\rangle$, we need to take into account the optical pumping of the system and the non-radiative decay of the S_1 state. To this end we append the following source and sink phenomenological terms to the equations of motion:

$$\left(\frac{\mathrm{d}}{\mathrm{d}t}n_{00_2}\right)_{\text{pump}} = p(t, \Delta t), \tag{8}$$

$$\left(\frac{\mathrm{d}}{\mathrm{d}t}n_{ab_1}\right)_{\text{decay}} = -\rho_{ab_1}\Gamma^{-1}, \tag{9}$$

where, $p(t)$ is the Gaussian or hyperbolic secant square function (Δt is the FWHM duration), and Γ is the empirical time scale of the non-radiative $S_1 \rightarrow S_0$ decay.

III. FITTING PROCEDURE AND STATIC PARAMETERS

The starting point for fitting the transient absorption (TA) spectra is the determination of the static model parameters. The static parameters govern the spectral shapes, as discussed in the main text. Firstly, we fit the absorption spectra using a simplex search method[4]. Secondly, using the absorption contour we subtract the ground state bleaching (GSB) contribution from the TA spectra at late times ($T > 1\,\text{ps}$) in the effort to separate the excited state absorption (ESA) contribution. Once we have the ESA contour we repeat the numerical fitting. The static parameters for both molecules determined by this procedure are given in Table S1.

Table S1. Static parameters of the transitions.

	carotenoid		β-carotene	
parameter	$S_0 \rightarrow S_2$	$S_1 \rightarrow S_n$	$S_0 \rightarrow S_2$	$S_1 \rightarrow S_n$
ω_{X} (cm^{-1})	19500	16800	19880	17350
$\Delta\omega_{\text{X}}$ (cm^{-1})	630	940	600*	800
d_α	0.83	0.33	0.9	0.27
d_β	0.83	0.15	0.64	0.27

*all the profile functions are Lorentzians, except for the linear absorption of β-carotene, which was best described by a Gaussian function

We then continue by fitting the dynamical parameters. One group of these parameters is responsible for the internal conversion process: $\omega^{(21)}$, $d_{ab}^{(21)}$, γ, λ_f. As an initial guess, we took from the literature the approximate values for the energy gap[5] and the displacements[6]. The internal conversion rates are then calculated to adjust λ and γ. We obtain the final values of the set by evaluating the time at which ESA is peaking. A note is due here that the set is not uniqly determined by the TA experiment and certain variation in these parameters might yield the same rate, therefore more precise values of the parameters should be determined by complementary experiments, such as by Polivka *et al.*[6]. Still, the obtained parameters are within a reasonable range and the corresponding rate is stable under their slight variation. Lastly, λ_c which governs the rate of vibrational relaxation is determined by matching the rise time of ESA.

IV. GLOBAL TARGET ANALYSIS

The GTA of transient absorption spectra of the carotenoid (which as defined in the main text refers to 7′-apo-7′-(4-aminophenyl)-β-carotene) and β-carotene are based on the approach described by van Stokkum et al.[7]. Assuming principal separability, a noise free time-resolved spectrum $\Psi(t, \lambda)$, is defined as a superposition of n_{comp} different components:

$$\Psi(t, \lambda) = \sum_{l=1}^{n_{comp}} c_l(t)\epsilon_l(\lambda),$$

where $c_l(t)$ is the concentration and $\epsilon_l(\lambda)$ is the spectrum of the component l. According to van Stokkum et al., without prior knowledge of a system, the first step is to fit the experimental data as a sum of exponential decays

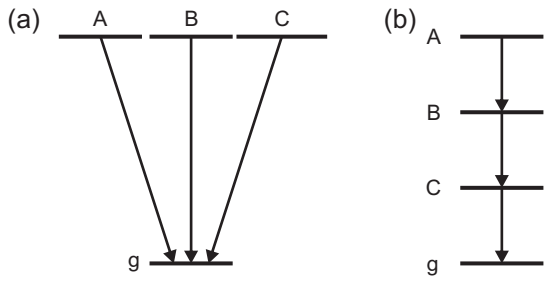

FIG. S1. Two simple kinetic models: (a) parallel and (b) sequential model.

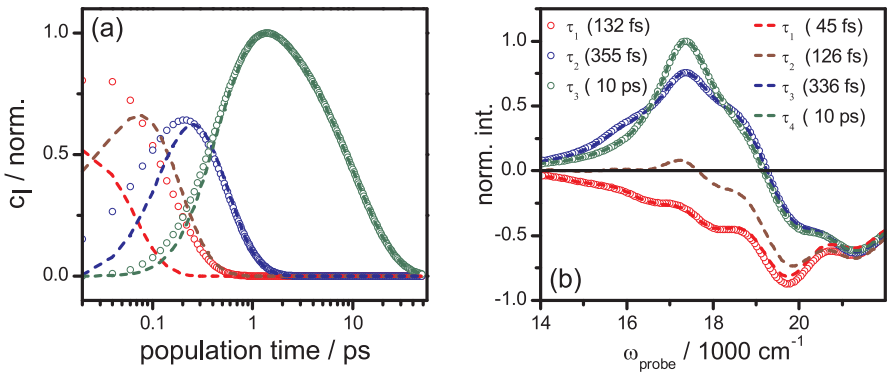

FIG. S2. (a) Concentration profile of 3-state (circle) and 4-state (dashed line) sequential models fitted to β-carotene simulated data. (b) The corresponding EAS.

adding additional time constants until the data is well described in terms of a nonlinear least square analysis. This can be considered by inspecting the simplest example of a parallel model with equal starting population in each component (Fig. S1(a)), the results of which are referred to as the decay associated spectra (DAS). The next simplest analysis employes a sequential model (Fig. S1(b)). The resultant outputs are referred to as the evolution associated spectra (EAS). We note that when the data is well described by both forms of analysis, the retrieved number of decays and different decay times should compare well. Significant deviation between these values indicates over-fitting of the data. It is then tempting to apply prior (and often biased) knowledge of the underlying structure of the population network in a targeted analysis (GTA) to retrieve so called state associated spectra (SAS).

In this work, we apply a simple sequential model ($1 \longrightarrow 2 \longrightarrow ... \longrightarrow n_{comp}$), convoluted with a Gaussian profile that describes the duration of the instrument response function, to analyze both experimental and modeled data. Our intent is to highlight the subtle differences between the two sets of data, which would be difficult to discuss on the basis of comparing just the simple kinetic traces (Fig. 4 of the main text). Note, here the term GTA is used in its most general form.

Figure S2 compares EAS for β-carotene simulated data, using a sequential model with 3 or 4 decays, respectively. Results for the simulated carotenoid data are not shown. For the 3-state model, we obtained three EAS with respective lifetimes of 132 fs, 355 fs, and 10 ps. As discussed in the main text, these components in combination with the determined lifetimes can be associated with the previously assigned S_2, hot-S_1 and S_1 states, respectively. This means that GTA, applied to simulated pump–probe data from our vibrational cooling model, reproduces the spectral signatures known from the experiment. When testing a 4-sate sequential model, we obtain three species with nearly identical features as compared to the 3-state model, i.e., S_2, hot-S_1 and S_1. The fourth component (brown dashed line in Fig. S2(b)), however, does not describe a long-lived S^*-like feature. Instead, the GTA algorithm delivers an additional short-lived species which appears to be the average between the first and the second species of the 3-state model. In the previous studies of carotenoids, such short-lived components were interpreted as additional intermediate states such as S_x[5,8]. This supports the above assertion that GTA is susceptible to over-fitting and furthermore, it is a typical example of GTA's inability to correctly describe the fast time-dependent spectral changes, such as those resulting from vibrational cooling[9].

In order to make a detailed comparison between the experimental and simulated results, both are analyzed using the sequential model described above. However, the simulated data are fit using only three states (for the reasons described above), while the experimental data require a minimum of four states for an adequate fit (Fig. S3). The

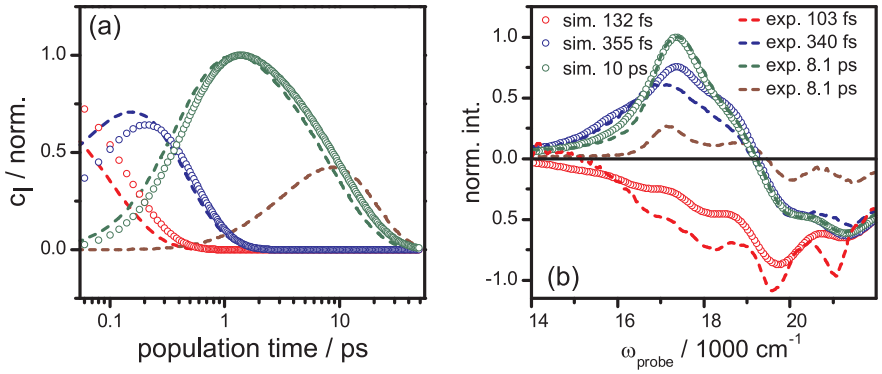

FIG. S3. Results for a 3-state sequential fit to β-carotene simulated data (circles) and a 4-state fit to experimental data (dashed lines). (a) Fitted concentration profiles. (b) The retrieved EAS.

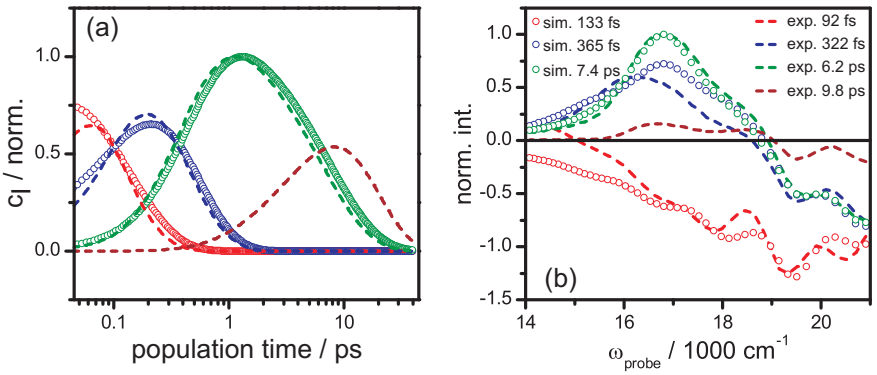

FIG. S4. Results for a 3-state sequential fit to the carotenoid simulated data (circles) and a 4-state fit to experimental data (dashed line). (a) Fitted concentration profiles. (b) The retrieved EAS.

first three species obtained for the experimental data are in good agreement with those obtained for the simulated data with lifetimes of 103 fs, 340 fs and 8.1 ps c.p.t. 132 fs, 355 fs, and 10 ps, respectively. The spectral shape and lifetime of these three states allow their ascription to species as follows: S_2 (red dashed line), hot-S_1 (green dashed line) and S_1 (blue dashed line). Simulation and experiment differ upon addition of a fourth state to the sequential model. Instead of adding an intermediate state between S_2 and hot-S_1, as shown for simulated data in Fig. S2, a 4-state model applied to experimental data delivers a long-lived component (8.1 ps, brown solid line in Fig. S3). This long lifetime in addition to the peak in the absorption at 18800 cm^{-1}, blue-shifted compared to the S_1-maximum, give this feature the properties of the S^* state. We note that the experimental results for β-carotene are also reproduced by a 3-state model. The point of the above discussion is to highlight that GTA gives different results for experiment and simulation, despite their generally good agreement when comparing traces at specific detection frequencies, as shown in Figure 4 of the main text. This highlights that GTA is a sensitive tool for model testing.

Equivalently to the treatment of β-carotene in Fig. S3, Fig. S4 compares simulated and experimental GTA results for the carotenoid. For the experimental data, we again obtain four different species, where the two long-lived components (green and brown solid lines) exhibit different lifetimes of 6.2 ps and 9.8 ps, respectively. For the carotenoid, the χ^2 values at the convergence (Table S2), confirm that three independent components are not enough to describe the experimental data.

Table S2. χ^2 values at the convergence of fitting procedure.

	β-carotene				carotenoid			
data	exp.		sim.		exp.		sim.	
#decays	3	4	3	4	3	4	3	4
χ^2	0.21	0.17	12.74	12.45	0.06	0.03	106.9	132.9

As was the case for β-carotene discussed in Fig. S3, the simulated data for the carotenoid do not support a component with a lifetime that is significantly longer than the lifetime of S_1, which was set phenomenologically to

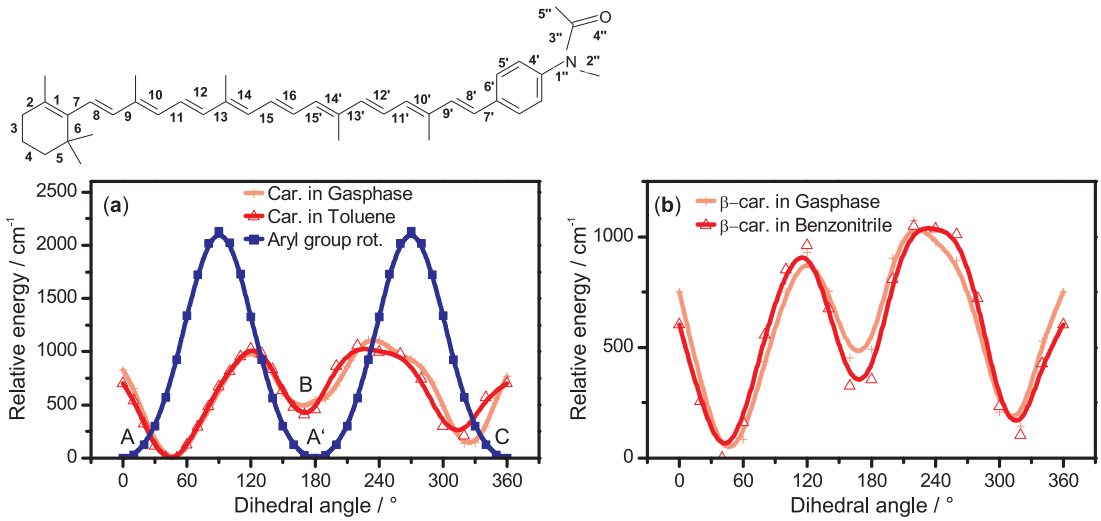

FIG. S5. The dependence of the relative electronic ground state B3LYP/def2-SV(P) energies on the torsional angles Θ_1 and Θ_2. The up triangles and crosses stand for the torsion of β-ionylidene moiety (bonds Nos. 1 and 7) and the squares mark torsion along the dihedral angle of phenyl-ring (bonds Nos. 1´ and 7´) in the carotenoid. The light-red line stands for the gas-phase calculations and the light-red line denotes calculations in the indicated solvent.

7.4 ps in the simulation. Therefore, GTA confirms that the vibrational structure of the ESA signal arising from the vibrational cooling model alone is not enough to explain S^*-related features in carotenoids with longer chain-length or for carotenoids where the conjugated π-electron system extends to the endgroups as discussed in this work. In such cases, the inhomogeneous ground state model provides a likely physical basis for all experimental findings, as discussed in the main text.

V. DETAILS ON QUANTUM CHEMICAL CALCULATIONS

The electronic ground state geometries of the studied molecules were optimized using the Density Functional Theory (DFT) employing Becke's three parameter hybrid functional and the Lee, Yang and Parr correlation functional (B3LYP)[10]. On the basis of B3LYP geometries, the single point Multireference Configuration Interaction (MRCI) calculations using the resolution of the identity (RI) approximation were performed for the selected CASSCF electron space (6 electrons and 7 molecular orbitals). All quantum chemical calculations were done using the ORCA program package[11] and the basis set def2-SV(P) was used[12]. Solvent effects were incorporated using the SMD solvation model[13]. The calculated molecules were visualized using the Molekel program package[14]. To investigate the inhomogeneous ground state model for the carotenoid and β-carotene, we performed quantum chemical calculations with the aim of identifying close-lying, thermally populated ground state conformers. The potential energy surface for rotation of the β-ionyliden endgroups in both molecules showed three possible conformations A, B, and C as indicated in Figure 6 of the main manuscript and in Fig. S5 below.

The inclusion of solvent effects, depicted by triangle symbols in Fig. S5, slightly modifies the barrier heights as well as the energies of local minima. During these calculations, the dihedral angle Θ_1 between the plane of the double bonds (bonds 1–7–8, see Fig. S5a) and the β-ionyliden-ring was rotated, while the geometry of the rest of the molecule was optimized. The relative energies for gasphase calculations with respect to the global minimum are depicted by cross-symbols in Fig. S5a and b, for the carotenoid and β-carotene respectively. The minima A, B, and C and their relation to S_1 and S^* are discussed in the main text. The potential for rotation of the phenyl endgroup, present in the carotenoid, is shown as the blue curve with square symbols in Fig. S5a. In this case, the torsional potential is more symmetric with only two minima, which is explained by the absence hindering methyl-groups on the phenyl-ring. The global minimum at 0° (A conformation) and the local minimum near 180° (A' conformation) are closer in energy than the two lowest lying minima for the rotation of the β-ionyliden fragment as shown in Table S3.

The main difference between conformers A and A' lies in the orientation of the –N(CH_3)CO-CH_3 group in the para position of benzene ring. In Table S3, this orientation is quantified by dihedral angle Θ_3 between bonds 1 and 2". Figure S6 shows the molecular structure and the electron densities of the global minimum, conformer A in Fig. S5, of the carotenoid (Fig. S6a) and β-carotene (Fig. S6b).

Table S3. Gas-phase dihedral angles and electronic B3LYP/def2-SV(P) energies for the conformations indicated in Fig. S5.

Conformation	Θ_1 / deg.	Θ_2 / deg.	Θ_3 / deg.	E_{B3LPY} / Hartree
A	46	1	151	–1683.678601
B	169	0	264	–1683.676668
C	313	0	62	–1683.677901
A'	45	180	295	–1683.678513

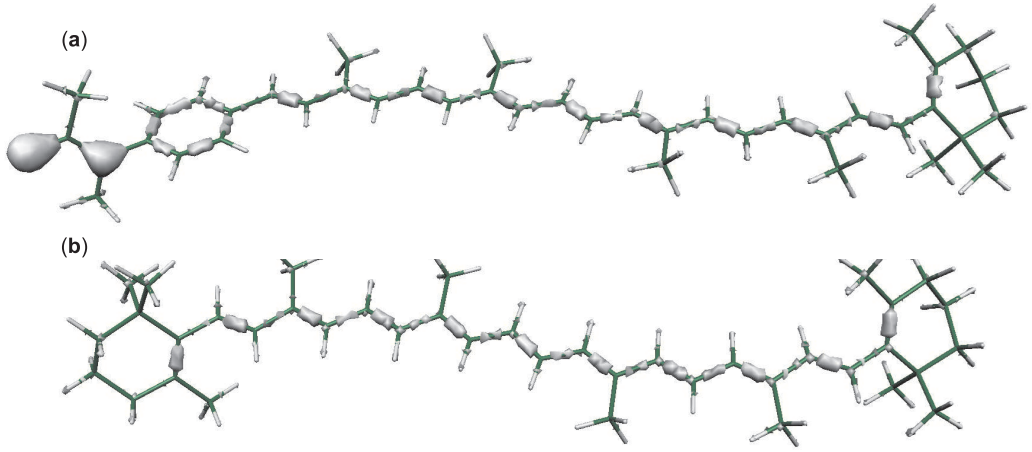

FIG. S6. B3LYP/def2-SV(P) ground state electron densities of the global minimum energy sturcture (conformer A) for a) the carotenoid and b) β-carotene. The densities are plotted for the isosurface 0.27 atomic units.

For the carotenoid depicted in Fig. S6a, the electron conjugation clearly extends towards the phenyl-ring, which explains the high barrier between the respective rotational conformers depicted in blue in Fig. S5a.

[1]A. E. Jailaubekov, M. Vengris, S.-H. Song, T. Kusumoto, H. Hashimoto and D. S. Larsen, *J. Phys. Chem. A*, 2011, 3905–3916.
[2]E. E. Ostroumov, G. M. Marc, M. Reus and A. R. Holzwarth, *J. Phys. Chem. A*, 2011, **115**, 3698–3712.
[3]L. Valkunas, D. Abramavicius and T. Mančal, *Molecular Excitation Dynamics and Relaxation*, Wiley-VCH, Weinheim, 2013.
[4]J. C. Lagarias, J. A. Reeds, M. H. Wright and P. E. Wright, *SIAM Journal on optimization*, 1998, **9**, 112–147.
[5]T. Polívka and V. Sunström, *Chem. Rev.*, 2004, **104**, 2021–2071.
[6]T. Polívka, D. Zigmantas, H. A. Frank, J. A. Bautista, J. L. Herek, Y. Koyama, R. Fujii and V. Sundström, *J. Phys. Chem. B*, 2001, **105**, 1072–1080.
[7]I. H. van Stokkum, D. S. Larsen and R. van Grondelle, *Biochimica et Biophysica Acta (BBA) - Bioenergetics*, 2004, **1658**, 262.
[8]H. Hashimoto, K. Yanagi, M. Yoshizawa, D. Polli, G. Cerullo, G. Lanzani, S. De Silvestri, A. T. Gardiner and R. J. Cogdell, *Archives of biochemistry and biophysics*, 2004, **430**, 61–9.
[9]H. Marciniak and S. Lochbrunner, *Chem. Phys. Lett.*, 2014, **609**, 184–188.
[10]A. D. Becke, *Journal of Chemical Physics*, 1993, **98**, 1372–1377.
[11]F. Neese, *Wiley Interdisciplinary Reviews: Computational Molecular Science*, 2012, **2**, 73–78.
[12]F. Weigend and R. Ahlrichs, *Physical Chemistry Chemical Physics*, 2005, **7**, 3297–3305.
[13]A. V. Marenich, C. J. Cramer and D. G. Truhlar, *Journal of Physical Chemistry B*, 2009, **113**, 6378–6396.
[14]P. Flukiger, H. P. Luthi, S. Sortmann and J. Weber, *Molekel 4.3*, Swiss National Supercomputing Centre, Switzerland, 2002.